



# Probing paracellular *-versus* transcellular tissue barrier permeability using a gut mucosal explant culture system

E. Michael Danielsen and Gert H. Hansen

Department of Cellular and Molecular Medicine, the Panum Institute, Faculty of Health Sciences, University of Copenhagen, Copenhagen, Denmark

## ABSTRACT

Intestinal permeation enhancers (PEs), i.e. agents improving oral delivery of therapeutic drugs with poor bioavailability, may typically act by two principally different mechanisms: to increase either transcellular -or paracellular passage across the epithelium. With the aim to define these different modes of action in a small intestinal mucosal explant system, the transcellular-acting PE sodium dodecyl sulfate (SDS) was compared to the paracellular-acting PE ethylenediaminetetraacetic acid (EDTA), using several fluorescent polar – and lipophilic probes. Here, SDS rendered the enterocyte cell membranes leaky for the relatively small polar tracers Lucifer yellow and a 3 kD Texas red-conjugated dextran, but most conspicuously SDS blocked constitutive endocytosis from the brush border. In contrast, the main action of EDTA was to increase paracellular passage across the epithelium of both polar probes, including 10 – and 70 kDa dextrans and lipophilic probes, visualized by distinct stripy lateral staining of enterocytes and/or accumulation in the lamina propria. In addition, EDTA caused a loss of epithelial cell polarity by opening tight junctions for diffusion of domain-specific basolateral/apical cell membrane protein markers into the opposite domains. By transmission electron microscopy, SDS caused the formation of vacuoles and vesicle-like structures at the lateral cell membranes. In contrast, EDTA led to a bulging of the whole enterocyte apex, resulting in a “cobblestone” appearance of the epithelium, probably caused by an extreme contraction of the perijunctional actomyosin ring. We conclude that the mucosal explant system is a convenient model for predicting transcellular/paracellular modes of action of novel prospective PEs.

## ARTICLE HISTORY

Received 14 February 2019  
Revised 26 March 2019  
Accepted 27 March 2019

## KEYWORDS

Intestinal permeation enhancers (PEs); ethylenediaminetetraacetic acid (EDTA); sodium dodecyl sulphate (SDS); small intestine; enterocyte; brush border

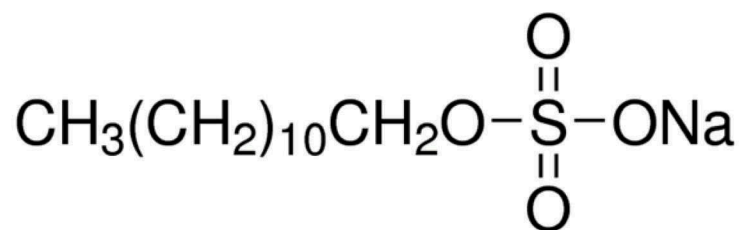
## Introduction

Intestinal permeation enhancers (PEs) are agents used to improve the oral delivery of therapeutic drugs with otherwise poor bioavailability in order to overcome the intestinal permeability barrier.<sup>1–3</sup>

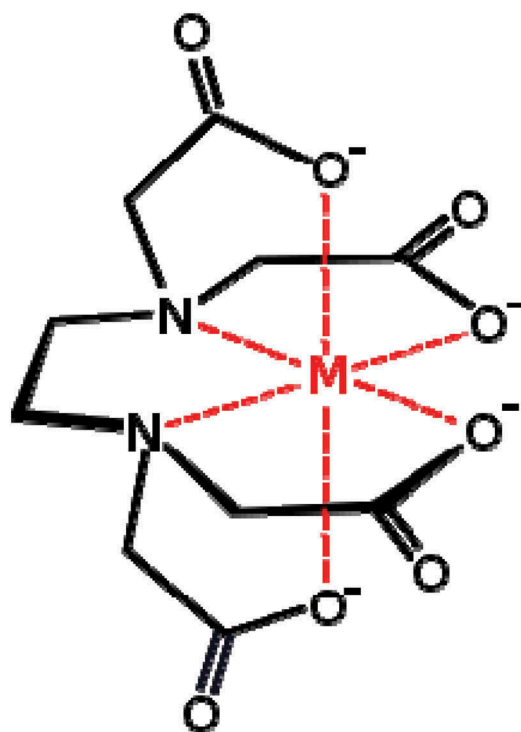
Under physiological conditions, this barrier acts as a strong selective filter to ensure efficient absorption of dietary nutrients, vitamins, and minerals whilst simultaneously preventing luminal pathogens from gaining entry into the organism.<sup>4,5</sup> Several components, including synthesis and luminal sequestering of antibodies, mucus and digestive enzymes, contribute to a strong combined defense of the host, but the ultimate obstacle preventing oral drugs from gaining access to the wider organism is the intestinal epithelium. Here, permeation must be achieved either by passage

through the epithelial cells (the transcellular pathway) or through the intercellular space between adjacent epithelial cells (the paracellular pathway), and different chemical properties are typically required of a prospective PE to enhance permeability across either of these two barriers. Consequently, PEs are typically classified as possessing a transcellular – or paracellular mode of action (or in some cases, a combination), according to their mode of action.<sup>6</sup>

Sodium dodecyl sulfate (SDS; [Figure 1](#)) belongs to the class of PEs having a transcellular mode of action, and like numerous other PEs in this class SDS is a soluble surfactant.<sup>6</sup> The majority of these types of agents are amphiphilic molecules capable to adsorb to epithelial cell membranes. Here, they insert into the outer leaflet of the bilayer, and by a flip-flop mechanism, they are capable of traversing the



Sodium dodecyl sulphate (SDS)



Ethylenediaminetetraacetic acid (EDTA)  
complexed to a metal cation

**Figure 1.** The chemical structure of EDTA and SDS. (The images were downloaded from [www.wikipedia.org](http://www.wikipedia.org) and [www.sigmaaldrich.com](http://www.sigmaaldrich.com), respectively.)

membrane. Exposure to such PEs typically renders the cell membrane more fluid and expands it, causing loss of integrity and subsequent increase in permeability.<sup>7</sup> At higher concentrations, surfactant type PEs may cause solubilization of membrane constituents and ultimately lysis of the cell membrane itself. Despite also being a strong protein denaturant,<sup>8</sup> SDS is widely used and characterized

as a PE with strong enhancement and slow recovery, and in a quantity up to 95 mg it is listed in the FDA Inactive Ingredients List.<sup>6</sup> As an alternative mechanism to membrane perturbation, transcellular permeation may be achieved by transcytosis from the gut lumen to the basolateral side of the epithelial cells. This pathway supposedly takes advantage of the natural route used in the uptake of maternal

immunoglobulins in the neonate,<sup>9</sup> and has been exploited to achieve transcellular transport of glucagon-like peptide 1 across epithelial cells.<sup>10,11</sup>

Ethylenediaminetetraacetic acid (EDTA; **Figure 1**) is a widely studied paracellular-acting PE by virtue of its ability to sequester divalent metal cations,<sup>12</sup> and it is characterized as a first generation tight junction (TJ) opener.<sup>6,13</sup> TJs are multimolecular protein complexes situated between adjacent enterocytes, strongly attaching them to one another so that only passage of water and low molecular weight solutes is permitted.<sup>14,15</sup> They present the main obstacle for drug permeation via the paracellular route although permeability through TJs can be modulated by physiological stimuli that operate via regulation of the contractility of the so-called perijunctional actomyosin ring (PAMR) to which TJs are intimately connected.<sup>16,17</sup> Control of PAMR tension by myosin light chain kinase (MLCK) phosphorylation of its substrate is thought to be dependent upon protein kinase C, the activation of which leads to phosphorylation (thereby causing inactivation) of MLCK and subsequent relaxation of PAMR.<sup>18</sup>

The present work aimed to study how two PEs with principally different modes of action, SDS and EDTA, affect uptake of a number of fluorescent polar – and lipophilic probes in cultured intestinal mucosal explants, a model system simple to use and more in-vivo-like than frequently used epithelial cell lines.<sup>19,20</sup> We found that different actions of SDS and EDTA regarding labeling patterns of enterocytes, paracellular space and lamina propria were easily visualized and distinguishable. Likewise, by transmission electron microscopy we showed that the two PEs affected the enterocyte cell membranes in a different manner at the ultrastructural level. We therefore recommend the mucosal explant system to be used as a convenient model in future studies assessing the mode of action employed by novel prospective PEs.

## Materials and methods

### Materials

The PE sodium dodecyl sulfate (SDS; molecular weight: 288) was supplied by Sigma-Aldrich ([www.sigmaaldrich.com](http://www.sigmaaldrich.com)), disodium ethylenediaminetetraacetic acid (EDTA; molecular weight: 372) by Merck

([www.merck.com](http://www.merck.com)), Lucifer yellow CH potassium salt (LY; molecular weight: 522), 3-kDa Texas red-conjugated dextran (TRD3), 10-kDa Oregon green-conjugated dextran (OGD10), 70-kDa Texas red-conjugated dextran (TRD70), fixable analogs of the FM lipophilic styryl dyes FM 1–43 (N-(3-triethylammoniumpropyl)-4-(4-dibutylamino) styryl pyridinium dibromide; molecular weight: 561), and FM 4–64 (N-(3-triethylammoniumpropyl)-4(6-(4-diethylamino) phenyl)-hexatrienyl) pyridinium dibromide; molecular weight: 789), Alexa 488-conjugated secondary antibodies for immunofluorescence microscopy, ProLong antifade reagent with DAPI, and a monoclonal antibody to Na<sup>+</sup>/K<sup>+</sup>-ATPase ( $\alpha$ -chain) from Thermo Scientific ([www.thermodanmark.dk](http://www.thermodanmark.dk)). Rabbit antibodies to pig intestinal aminopeptidase N (ApN) and sucrose-isomaltase (SI) were described previously.<sup>21,22</sup>

### Animals

Animal experimentation in Denmark is subject to ethical evaluation by the Ministry of Justice's Council for Animal Experimentation. Animal experimentation included in this work was performed only by licensed staff at the Department of Experimental Medicine, the Panum Institute, University of Copenhagen, and was covered by license 2012-15-2934-00077 issued to the Dept. of Experimental Medicine.

Segments of porcine jejunum, taken about 2 m from the pylorus of overnight fasted, postweaned animals, were surgically removed from the anesthetized animals. After excision of the tissue, the animals were sacrificed by an injection with pentobarbital/lidocaine (1 mg/kg bodyweight). As this study contained no further animal experimentation, no specific approval by an ethics committee was required. A total number of five post-weaned pigs were included in the present study.

### Organ culture of pig jejunal mucosa

Organ culture of intestinal tissue was performed essentially as described previously.<sup>23</sup> Briefly, after removal from the animals, jejunal segments (~20 cm) were quickly cut open longitudinally and placed in ice-cold RPMI medium. Mucosal tissue specimens weighing ~0.1 g were excised with a

scalpel and transferred to metal grids in organ culture dishes to which 1 ml of RPMI medium was added. The dishes were placed in an incubator kept at 37°C and subjected to 15 min of preincubation without any additions to the medium. SDS or EDTA was added to the culture medium at a final concentration of 0.05%. The following fluorescent probes for cellular uptake were added together with the PEs: LY (0.5 mg/ml), TRD3 (0.05 mg/ml), OGD10 (0.25 mg/ml), TRD70 (1.25 mg/ml), FM 1–43 (0.01 mg/ml) and FM 4–64 (0.01 mg/ml).

After addition of the above reagents, the explants were cultured in the presence of the probes for 1 h at 37°C, and after culture they were carefully rinsed in fresh medium and immersed in a fixative overnight at 4°C.

### Fluorescence microscopy

Explants were fixed at 4°C overnight in 4% paraformaldehyde in 0.1 M sodium phosphate, pH 7.2 (buffer A). Following fixation and a quick rinse in buffer A, the explants were immersed overnight in 25% sucrose in buffer A before mounting in Tissue-Tek and sectioning (~7 µm thick sections cut parallel to the crypt-villus axis) at –19°C in a Leica CM1850 cryostat. For immunolabeling, the sections were incubated for 1 h at room temperature with antibodies to ApN (diluted 1:2000), SI (diluted 1:2000) or Na<sup>+</sup>/K<sup>+</sup>-ATPase (diluted 1:100) in 50 mM Tris-HCl, 150 mM NaCl, 0.5% ovalbumin, 0.1% gelatin, 0.2% teleostan gelatin, 0.05% Tween 20, 0.05% Triton X-100, pH 7.2 (buffer B). Incubation with Alexa 488-conjugated secondary antibodies (diluted 1:200) was performed for 1 h at room temperature in buffer B.

Controls with omission of primary antibodies were routinely included in the labeling experiments.

Hematoxylin-eosin staining of fixed tissue sections was performed according to a standard protocol.

All sections were finally mounted in antifade mounting medium with DAPI and examined in a Leica DM 4000B microscope fitted with a Leica DFC495 digital camera. Images were obtained using Leica HCX PL Fluotar objectives with the following magnification/numerical aperture: 20 × /0.40, 40 × /0.65, 63 × /0.90, and 100 × /1.30. The following filter cubes were used: I3 (band-pass filter, excitation 450–490 nm), TX2

(band-pass filter, excitation 560/40 nm), and A4 (band-pass filter, excitation 360/40 nm).

### Electron microscopy

Cultured mucosal explants for electron microscopy were fixed in 3% glutaraldehyde (v/v), 2% (w/v) paraformaldehyde in buffer A overnight at 4°C. After a rinse in buffer A, the explants were post-fixed in 1% osmium tetroxide in buffer A for 1 h at 4°C, dehydrated in acetone and finally embedded in Epon. Ultrathin sections were cut in a Pharmacia LKB Ultratome III, stained with 1% (w/v) uranyl acetate in H<sub>2</sub>O and lead citrate, and finally examined in a Zeiss EM 900 electron microscope equipped with a Mega View II camera.

### Preparation of microvillus membrane vesicles and treatment with PEs

For the preparation of microvillus membrane vesicles pig, jejunal mucosa was fractionated by the divalent cation precipitation method.<sup>24</sup> Briefly, the mucosa was scraped from the gut and homogenized in 10 volumes of 2 mM Tris-HCl, 50 mM mannitol, pH 7.1, containing 10 µg/ml aprotinin and leupeptin. After centrifugation at 500 g, 5 min, MgCl<sub>2</sub> was added to the supernatant (final concentration: 10 mM), and after 10 min on ice, the preparation was centrifuged at 1.500 g, 10 min. The Mg<sup>2+</sup>-precipitated pellet (containing intracellular- and basolateral membranes) was discarded, and the resulting supernatant centrifuged at 48.000 × g, 30 min, to yield a pellet of microvillus membrane vesicles that was stored at –20°C until use.

For subsequent treatment with PEs, microvillus vesicles (~1 mg/ml) were resuspended in 25 mM HEPES-HCl, 150 mM NaCl, pH 7.1, and samples of 75 µl were mixed with 25 µl of SDS or EDTA to yield a final PE concentration range of 0–0.2% and 0–0.5 %, respectively. After 10 min incubation at 37°C and rapid cooling on ice, the vesicle suspensions were centrifuged at 25.000 × g, 10 min, to yield a membrane pellet of insoluble membrane protein and a supernatant of solubilized protein. Both fractions were collected and subjected to SDS/PAGE in 10% gels as described by Laemmli.<sup>25</sup> After electrophoresis and electrotransfer

onto Immobilon membranes, the protein was visualized by staining with Coomassie brilliant blue.

## Results

### **Actions of SDS and EDTA on the brush border membrane and on the epithelial morphology of cultured mucosal explants**

SDS and EDTA (Figure 1) were chosen in the present study as model PEs because of their well-known transcellular – or paracellular modes of PE action, respectively.<sup>6</sup> To establish optimal conditions for their use in the mucosal explant culture system, the solubilizing action of SDS and EDTA on isolated microvillus membrane vesicles was first determined. As shown in Figure 2, SDS solubilized microvillus proteins from the membrane in a concentration-dependent manner: at 0.025% (0.87 mM) only negligible amounts of proteins were released, whereas at 0.2% (6.9 mM), only small amounts remained insoluble in the pellet fraction. EDTA, on the other hand, did not cause any release of proteins from the microvillus membrane vesicles when used at concentrations up to 0.5% (13.4 mM). SDS is a powerful anionic detergent and protein denaturant with a critical micelle concentration of ~8 mM,<sup>8</sup> i. e. above the concentration range used here, so its strong solubilizing effect on microvillus membranes was predictable. Likewise, the absence of protein solubilization by EDTA agrees well with that of a compound lacking surfactant activity. In subsequent culture experiments both PEs were used at a concentration of 0.05% (1.73 mM SDS; 1.34 mM EDTA, a value well within the range previously used in other *in situ* -and *in vitro* studies.<sup>6</sup> In addition, a fixed culture period of 1 h was chosen for all experiments performed. This time period proved optimal for detecting immediate effects of the PEs on parameters such as apical endocytic activity, cell membrane leakage, and paracellular permeation, rather than recording accumulated long-term effects.

Figure 3 shows how exposure for 1 h to 0.05% SDS or EDTA affected the epithelial morphology of cultured mucosal explants. For both PEs, overall tissue architecture including epithelial integrity was generally well preserved, with the exception of the villus tips where foci of denudation were frequently observed, both with SDS and EDTA. Exfoliation of

senescent enterocytes normally takes place at the villus tip, but this is also a site where barrier restitution rapidly occurs after epithelial injury.<sup>26–28</sup> In addition to this effect EDTA, but not SDS, frequently caused the apex of the enterocytes to bulge into the lumen, creating a characteristic “cobblestone” appearance of the epithelial surface (Figure 3d). In the uptake experiments presented below, we mainly focused on how SDS and EDTA acted on the more well-preserved parts of the villus epithelium, that is, the enterocytes lining the sides of the villi rather than at the tip.

### **SDS and EDTA effects on localization of basolateral – and apical cell surface markers**

In control explants, antibodies to the Na<sup>+</sup>/K<sup>+</sup>-ATPase exclusively labeled the basolateral sides of the enterocytes, whereas the labeling using antibodies to the two prominent brush border enzymes aminopeptidase N (ApN) and sucrose-isomaltase (SI) was confined to the apical cell surface (Figure 4). This pattern of cell membrane protein distribution demonstrates the strict maintenance of cell polarity normally upheld in intestinal epithelial cells.<sup>29,30</sup> SDS did not affect the localization of any of the cell surface markers used, indicating that this transcellular-acting PE leaves cell polarity intact (Figure 4). In the presence of EDTA, on the other hand, patchy labeling for Na<sup>+</sup>/K<sup>+</sup>-ATPase was clearly visible at the apical surface of enterocytes and conversely, distinct traces of both ApN and SI were detectable along the lateral sides of the cells (Figure 4). This surprising result shows that the paracellular-acting PE EDTA is capable of disrupting the cell polarity of enterocytes, most likely by permitting diffusion of membrane proteins through the normally impenetrable TJs.

### **Actions of SDS and EDTA on epithelial permeability of polar probes**

LY is a small polar probe normally non-permeable to cell membranes.<sup>31</sup> It has previously been used to determine paracellular permeability in Caco-2 monolayers,<sup>32</sup> and we have used it in the mucosal explant organ culture system for studying epithelial permeability.<sup>33–35</sup> In control explants cultured in the presence of LY for 1 h, uptake into distinct subapical

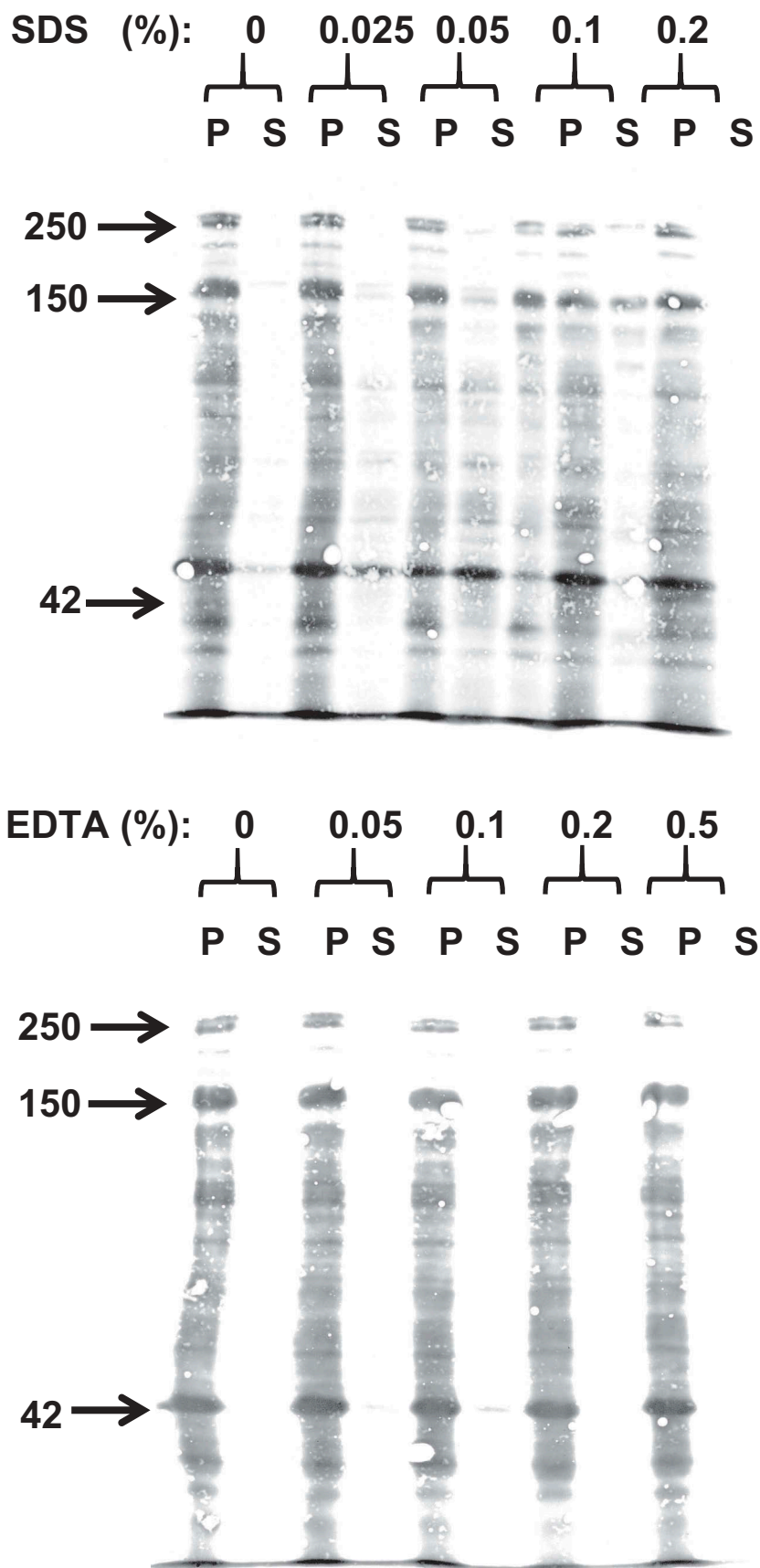


**Figure 2.** Extraction of microvillus membrane vesicles by SDS (top) or EDTA (bottom). Following their preparation, the microvillus membranes were extracted with the respective PEs at the indicated concentrations. After incubation and centrifugation, pellet (P) – and supernatant (S) fractions were analyzed by SDS/PAGE. Total protein was visualized by staining with Coomassie brilliant blue. Arrows indicate molecular weight-values of sucrose-isomaltase (250 kDa), aminopeptidase N (150 kDa) and actin (42 kDa).

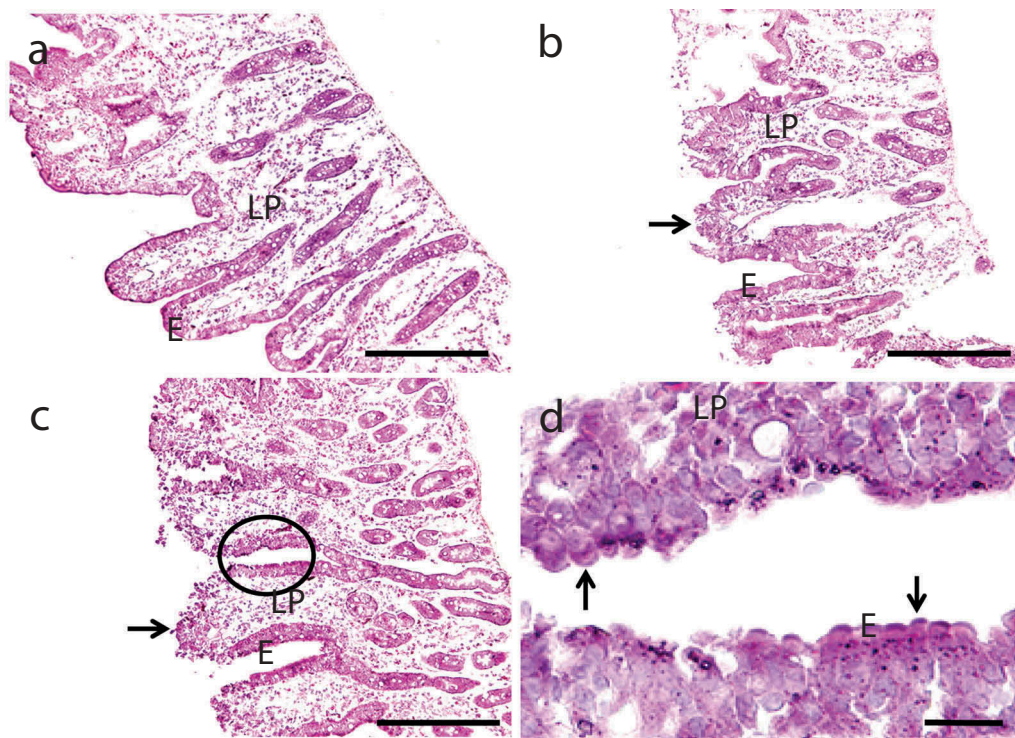


**Figure 3.** Hematoxylin-eosin stained sections of mucosal explants cultured for 1 h in the absence (a) or presence of 0.05% SDS (b) or 0.05% EDTA (c), as described in Methods. Both SDS and EDTA caused denudation at the tip of the villi (arrows in (b) and (c)), but the epithelium along the sides of villi and in the crypts was generally well preserved. (d) is a higher magnification image of the area circled in c and shows the characteristic “cobblestone” appearance of enterocytes caused by EDTA. Enterocytes (E) and lamina propria (LP) are indicated. Bars: 100  $\mu\text{m}$  (a–c); 20  $\mu\text{m}$  (d).

punctae just below the brush border of enterocytes could be seen (Figure 5), as previously observed. These punctae represent early endosomes localized in the terminal web region of enterocytes (hence termed “TWEES” for “terminal web early endosomes”), and they have previously been identified in these cells as early endosome antigen-1 (EEA-1)-positive structures.<sup>36,37</sup> Otherwise, the cytoplasm of the enterocytes was largely devoid of staining, indicating that LY did not penetrate through leaks in the cell membranes during culture. Stripy labeling of the intercellular space along the lateral sides of the epithelial cells and accumulation in areas of the subepithelial lamina propria is evidence that the tight junctions between adjacent enterocytes allow paracellular passage of this small polar probe across the epithelial barrier.

Dextrans are water soluble, hydrophilic polysaccharides commercially available in various molecular sizes. As fluorescent conjugates, they are useful polar probes due to their uncommon poly-( $\alpha$ -D-1,6-glucose) linkages, which render them resistant

to cleavage by most endogenous cellular glycosidases. In control explants, TRD3 labeled the enterocyte brush border well by 1 h, but unlike LY it was not taken up by endocytosis into TWEES, indicative of selectivity with regard to cargo in this process (Figure 5). Although lateral labeling along the enterocytes was not readily detectable, some patchy staining of the lamina propria implied a modest paracellular passage of TRD3 across the epithelium.

As shown in Figure 5, SDS essentially prevented both endocytic uptake of LY and binding to the brush border of TRD3. In addition, a diffuse staining of the enterocyte cytosol indicated leaks caused by loss of cell membrane integrity, but no conspicuous increase in lateral and/or lamina propria staining was apparent. Unlike SDS and despite the striking “cobblestone” appearance of the enterocytes, EDTA did not seemingly prevent endocytosis of LY or brush border binding of TRD3 (Figure 5). However, the subapical localization of the TWEES appeared disorganized compared to the control, and basolateral – and lamina propria

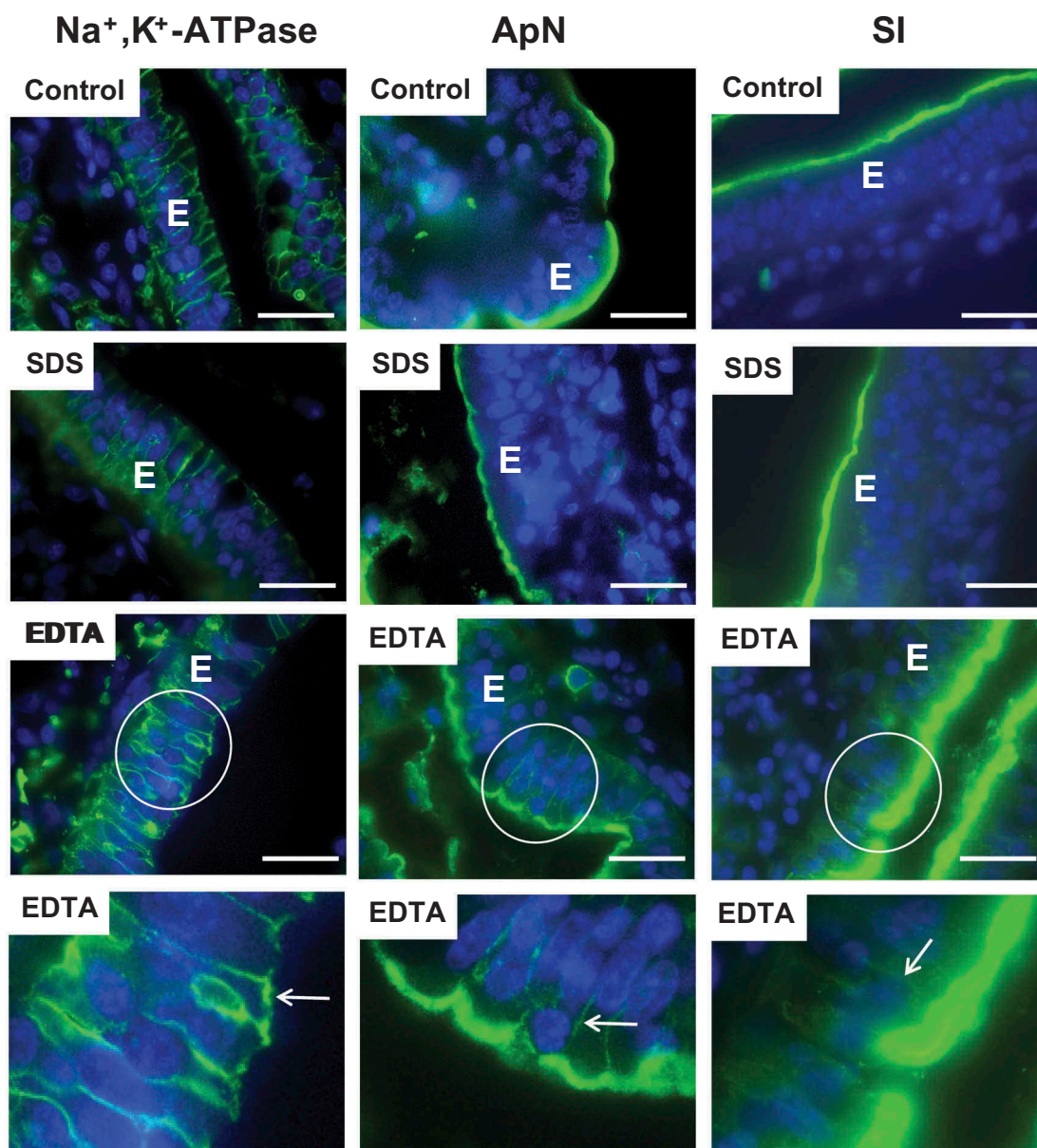


**Figure 4.** Effects of SDS and EDTA on surface expression of enterocyte cell membrane markers. Sections of mucosal explants, cultured for 1 h in the absence (Control) or presence of 0.05% SDS or 0.05% EDTA, were immunolabeled for the basolateral marker  $\text{Na}^+/\text{K}^+$ -ATPase or the apical markers ApN or SI. Membrane polarity of all three markers was unaffected by SDS, but EDTA caused a patchy apical appearance of  $\text{Na}^+/\text{K}^+$ -ATPase as well as a distinct lateral labeling of both ApN and SI. (The bottom panel shows enlarged images of the respective circled areas. Arrows indicate areas of mislocated markers. Bars: 20  $\mu\text{m}$ .)

staining with TRD3 indicated an increased paracellular permeability of this probe.

Figure 6 shows that the two dextrans of larger size, OGD10 and TRD70, bound well to the enterocyte brush border of the control without being taken up by endocytosis. Lateral staining was not detectable, but faint TRD70-staining of the lamina propria was suggestive of a modest paracellular uptake. In the presence of SDS, brush border

binding was either absent or diminished, but faint basolateral – and lamina propria staining indicated some paracellular passage of both OGD10 and TRD70 through the epithelium. However, by comparison the accumulation of both probes in the lamina propria caused by EDTA was far more pronounced, demonstrating the marked enhancement of paracellular permeability of macromolecules in the 10–70 kDa range.

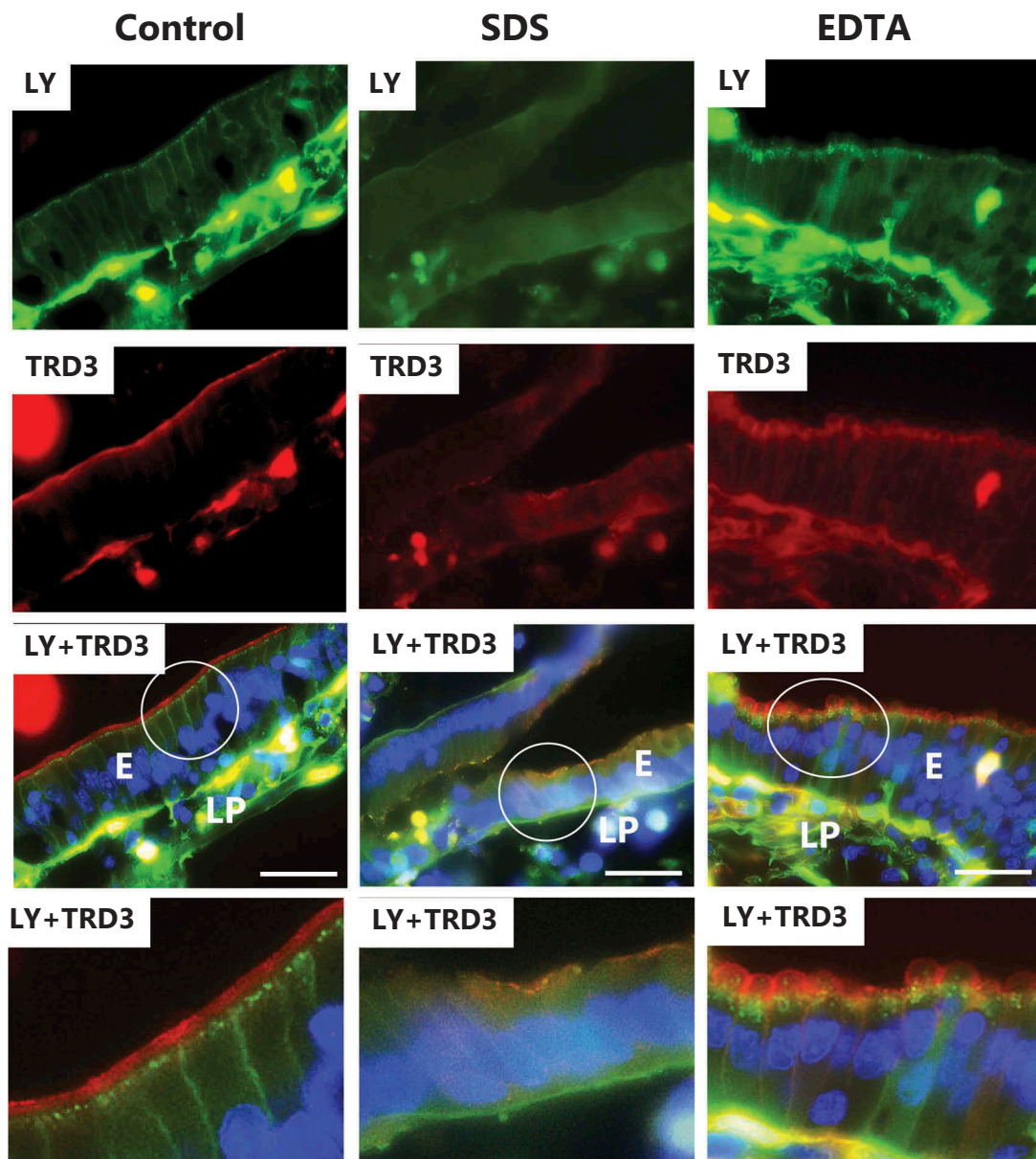


**Figure 5.** Effects of SDS and EDTA on the permeability of the polar probes LY and TRD3. Images of sectioned mucosal explants cultured for 1 h in the presence of LY and TRD3. The bottom panel shows enlarged images of the respective circled areas. Bars: 20  $\mu$ m.

### ***Actions of SDS and EDTA on the interaction of lipophilic probes with the brush border membrane***

FM dyes are non-toxic, water-soluble and lipophilic membrane probes that only become fluorescent when incorporated into cell membranes.<sup>38</sup> As shown in Figure 7, FM 1–43 labeled the entire brush border of control enterocytes, but after 1 h of culture it most strongly appeared in a string of subapical punctae, much like LY (Figure 5), and thus further evidence of a rapidly ongoing constitutive apical endocytosis into TWEEs. In addition, this FM dye stained the

interior of goblet cells, as previously observed.<sup>36</sup> FM 1–43 and FM 4–64 have identical triethylammonium-propyl polar headgroups, but FM 4–64 has the longest lipophilic tail with six instead of two conjugated carbon atoms separating the two aromatic rings. FM 4–64 strongly labeled the entire brush border, but subapical punctae were relatively faint, compared with those visualized by FM 1–43, thus showing a relatively slower uptake of this FM dye into TWEEs, as also earlier observed.<sup>39</sup> Unlike LY, none of the two FM dyes stained the lamina propria or the basolateral cell membranes of the enterocytes, indicating that

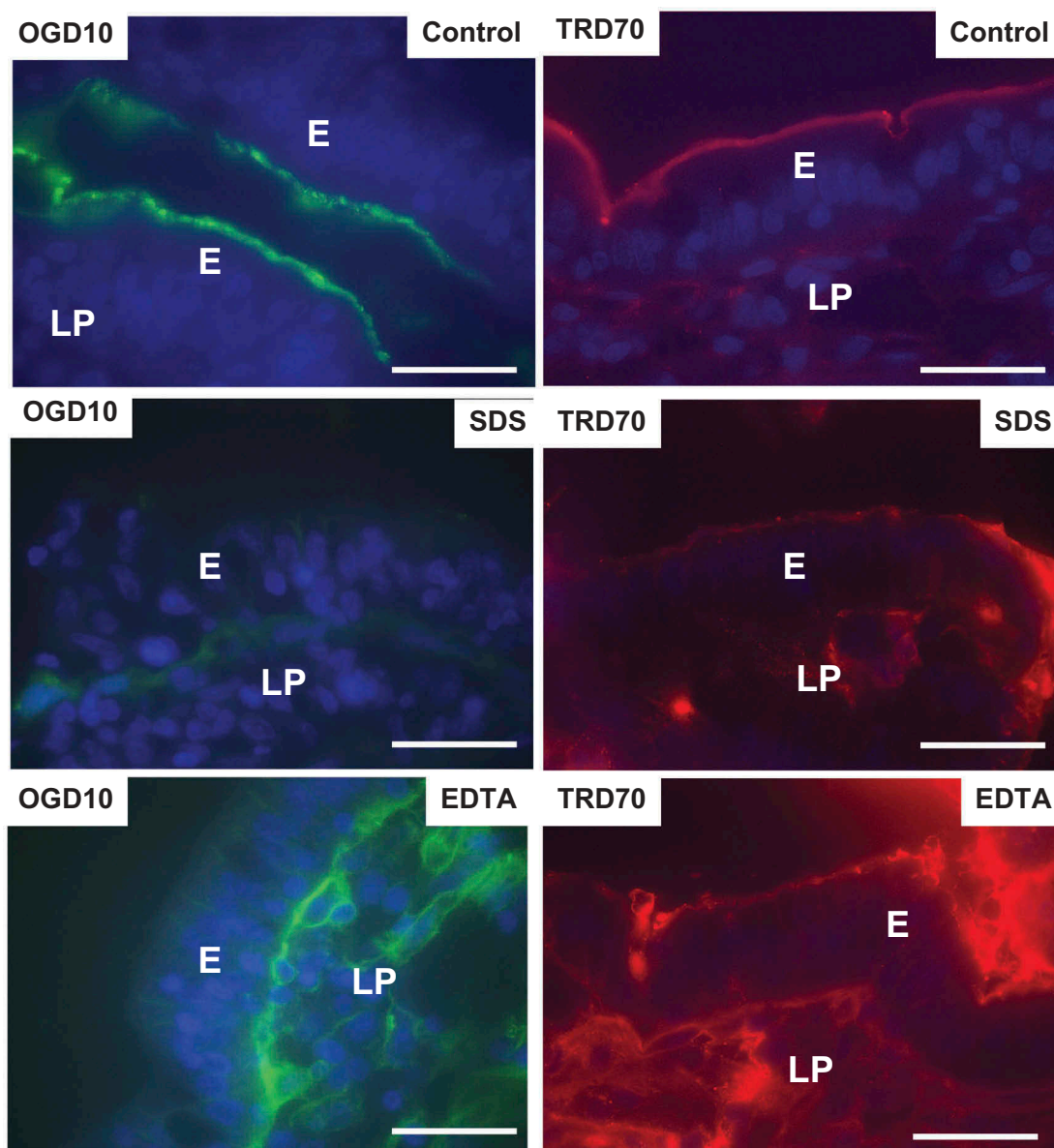


**Figure 6.** Effects of SDS and EDTA on the permeability of the polar probes OGD10 and TRD70. Images of sectioned mucosal explants cultured for 1 h in the presence of OGD10 or TRD70. Bars: 20  $\mu$ m.

these lipophilic probes are incapable of passing the TJ complexes in the control situation.

In the presence of SDS, little or no uptake of FM 1–43 or FM 4–64 into TWEEs was observed (Figure 7), indicating a blockage of apical endocytosis, as also observed with LY. A faint, diffuse staining of the enterocyte cytosol by FM 1–43 was suggestive of some leakage through the cell membranes, but stripy basolateral staining or accumulation in the underlying lamina propria was not detected, indicating well-preserved tight junctions in the presence of SDS.

In contrast, endocytosis of FM dyes into punctae in the bulging subapical region still occurred in the

presence of EDTA (Figure 7). In addition, a mosaic pattern of leaky enterocytes was observed, most clearly seen with FM 1–43, and both FM dyes could also be seen in the lamina propria, suggesting an opening of the paracellular route for these lipophilic probes.

#### ***Actions of SDS and EDTA on the ultrastructure of the enterocyte cell membranes***

At the ultrastructural level of transmission electron microscopy, the enterocyte brush border of control explants cultured for 1 h appeared as tightly packed microvilli of uniform length and diameter, and the TJ

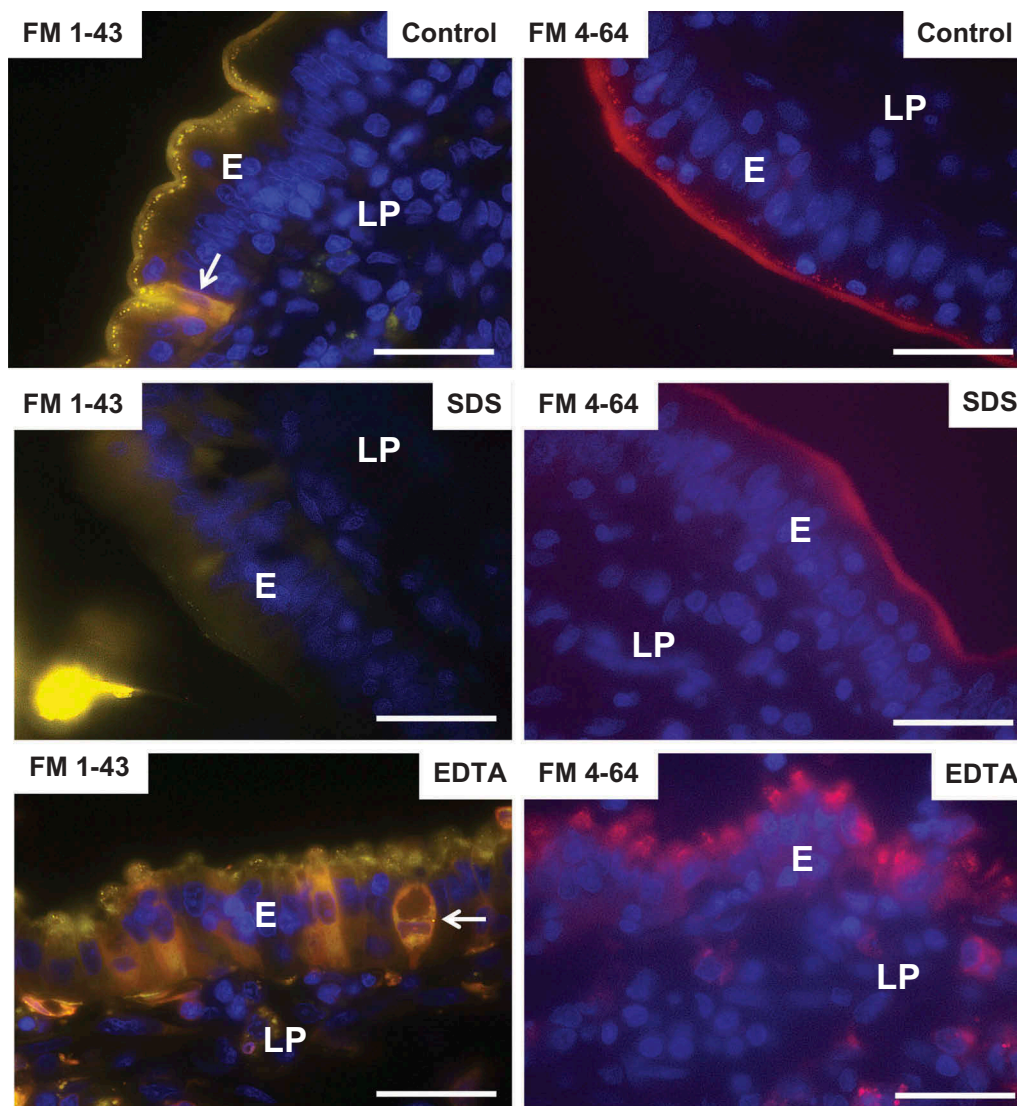


**Figure 7.** Effects of SDS and EDTA on the permeability of the lipophilic membrane probes FM 1–43 and FM 4–64. Images of sectioned mucosal explants cultured for 1 h in the presence of FM-1–43 and FM-4–64. (FM-1–43-positive goblet cells are indicated by arrows). Bars: 20  $\mu$ m.

complexes between adjacent cells typically appeared as characteristic electron-dense structures (Figure 8). The observed effect of SDS was a moderate decrease in microvillus density and length, apparent in longitudinal views, whereas in cross sections the microvilli were normal, apart from irregular shapes occasionally seen. In addition, microvesiculation of microvilli was seen more frequently than in controls (Figure 8). TJs were seemingly unaffected by SDS, but the lateral enterocyte cell membranes were perturbed (Figure 9). Thus, instead of the normal meandering and narrow intercellular space between adjacent cells,

vacuoles filled with numerous vesicle-like structures were frequently observed.

In the presence of EDTA, microvilli appeared less organized both in longitudinal – and cross sections, most likely because of the induced contraction of the PAMR in the terminal web, causing the bulging of the apical part of the enterocytes and a resulting “fanning” of the microvilli (Figure 8, 9). With regard to TJ complexes, they appeared morphologically unaffected in enterocytes showing only a modest bulging of the cell apex, whereas in cells displaying extreme bulging, TJs seemed to be missing altogether (Figure 9).

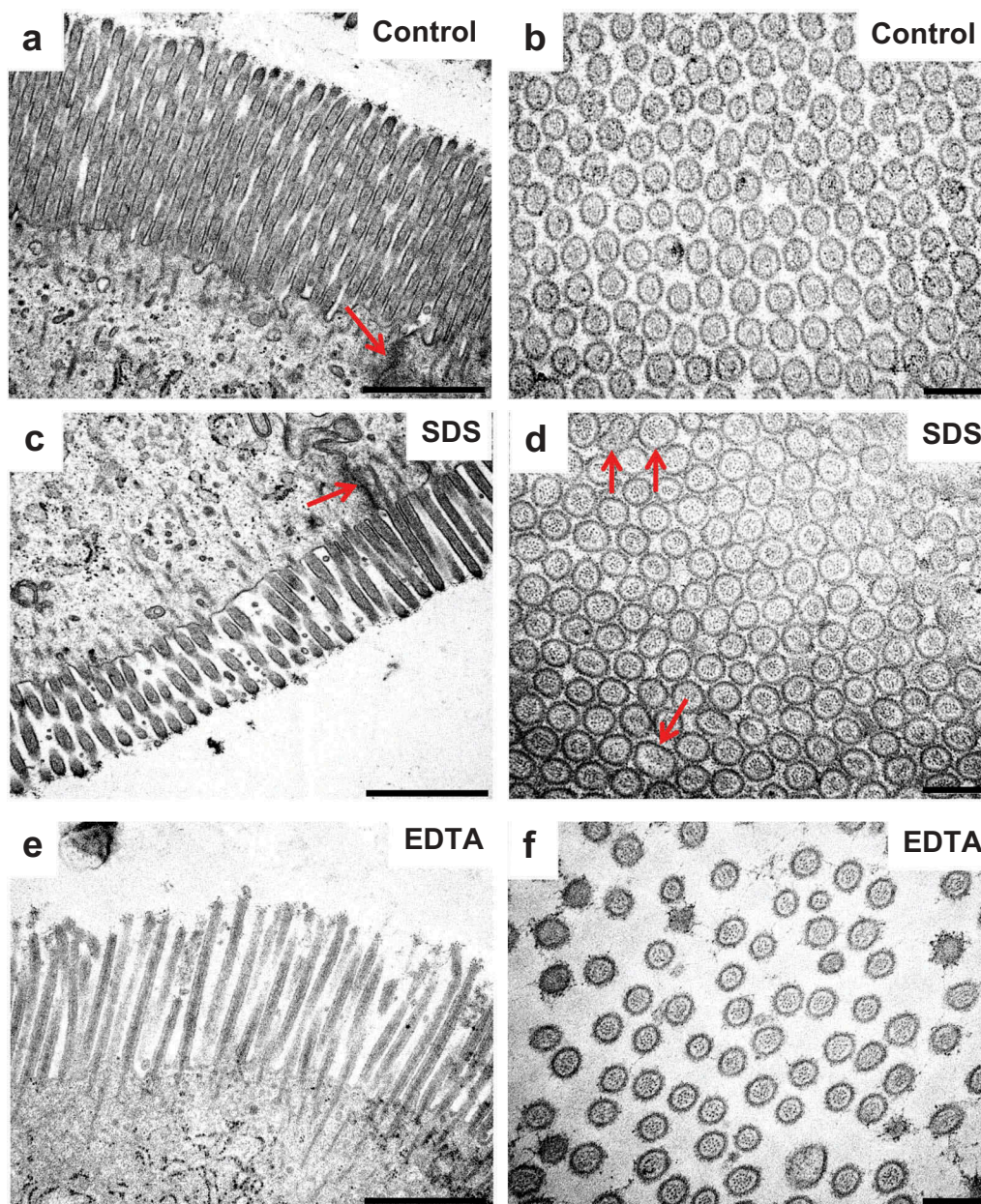


**Figure 8.** Effects of SDS and EDTA on the enterocyte ultrastructure I. Electron micrographs of epon sections of mucosal explants cultured for 1 h. The images show microvilli in longitudinal – and cross sections. Arrows indicate TJs in (a) and (c) and irregular-shaped microvilli in (d). Bars: (a,c,e): 1  $\mu\text{m}$ ; (b,d,f): 0.2  $\mu\text{m}$ .

## Discussion

In the present work, we have compared the actions of two well-known transcellular – and paracellular PEs in a mucosal explant system, using a total of six fluorescent probes, four of which were polar of varying size and two lipophilic having membrane-interacting properties. Collectively, these probes allowed an assessment of a potential PE effect based on the following parameters: Paracellular permeation (increased lateral – and lamina propria

staining), and epithelial cell permeation (altered endocytic uptake; induction of membrane leaks). A summary of the results is presented in [Table 1](#). The polar probes used, LY and fluorescence-conjugated dextrans in the size range of 3–70 kDa, visualized well the changes in paracellular passage across the epithelium by showing a distinct stripy staining along the lateral sides of the enterocytes and accumulation in the underlying lamina propria. In controls, LY was easily detected in both these locations whereas the larger dextrans

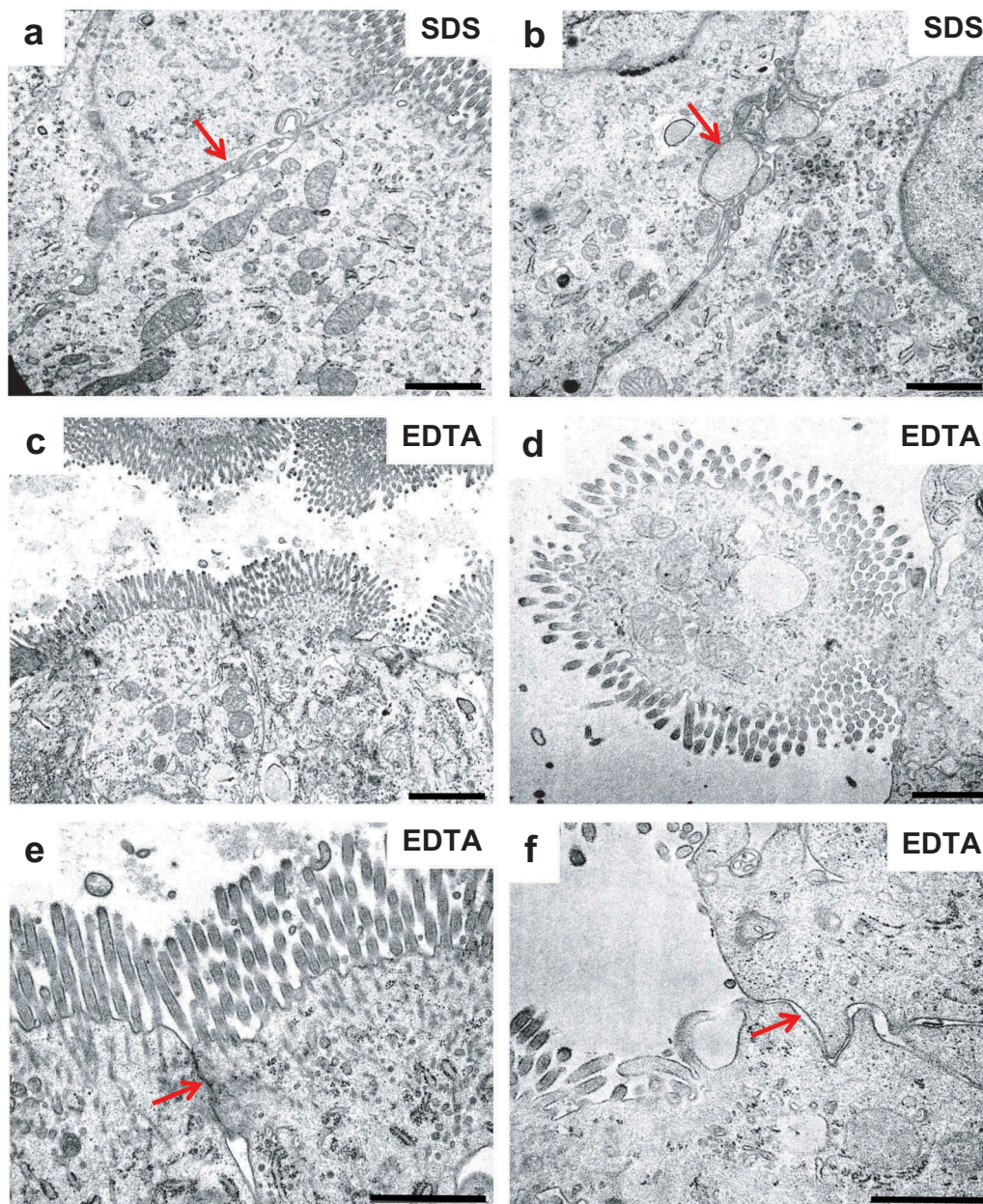


**Figure 9.** Effects of SDS and EDTA on the enterocyte ultrastructure II. Electron micrographs of epon sections of mucosal explants cultured for 1 h. (a,b): Arrows indicate vesicles and vacuoles along the lateral enterocyte cell membranes generated by SDS. (c,d): Enterocytes displaying moderate (c) or extreme (d) bulging into the lumen after exposure to EDTA. (e,f): Cell contacts between adjacent enterocytes with the TJ complex either preserved (arrow in (e)) or missing (arrow in (f)) after exposure to EDTA. Bars: 1  $\mu$ m. Electron micrograph showing three adjacent enterocytes of a jejunal mucosal explant cultured for 1 h in the presence of 0.05% EDTA. The vigorous contraction of the subapical perijunctional actomyosin ring caused the whole brush border to pinch off from the enterocyte in the middle.

typically displayed only poor transepithelial permeability. EDTA exhibited marked paracellular PE action on all three dextrans, in clear contrast to SDS that had only little or no effect. Regarding the lipophilic probes FM 1-43 and FM 4-64, they were less useful as predictors of paracellular PE action, although EDTA did cause a slight staining

in the lamina propria. More impressive was the detection of both apical  $\text{Na}^+/\text{K}^+$ -ATPase and lateral ApN and SI. Such a loss of cell polarity has not to our knowledge been reported earlier, but it is supported by the apparent lack of TJ complexes, observed by electron microscopy of severely affected enterocytes displaying extreme bulging,

**Table 1.** Overview of observed PE actions of SDS and EDTA studied in a mucosal explant system using fluorescent polar – and lipophilic probes. In all experiments performed jejunal mucosal explants were cultured for 1 h in the absence (controls) or presence of SDS or EDTA at a final concentration of 0.05%. The fluorescent probes were added together with the PEs at the following concentrations: LY (0.5 mg/ml), TRD3 (0.05 mg/ml), OGD10 (0.25 mg/ml), TRD70 (1.25 mg/ml), FM 1–43 (0.01 mg/ml) and FM 4–64 (0.01 mg/ml).

| Probe        | PE actions              |                  |              |                         |                  |   |
|--------------|-------------------------|------------------|--------------|-------------------------|------------------|---|
|              | SDS                     |                  |              | EDTA                    |                  |   |
|              | Paracellular permeation | Cellular effects |              | Paracellular permeation | Cellular effects |   |
| Endo-cytosis |                         | Membrane leaks   | Endo-cytosis |                         | Membrane leaks   |   |
| LY           | ↔                       | ↓↓↓              | ↑            | ↑                       | ↔                | ↑ |
| TRD3         | ↔                       | ↔                | ↑            | ↑↑↑                     | ↔                | ↑ |
| OGD10        | ↑                       | ↔                | ↔            | ↑↑↑                     | ↔                | ↔ |
| TRD70        | ↑                       | ↔                | ↔            | ↑↑↑                     | ↔                | ↔ |
| FM 1–43      | ↔                       | ↓↓↓              | ↔            | ↑                       | ↔                | ↑ |
| FM 4–64      | ↔                       | ↓↓↓              | ↔            | ↑                       | ↔                | ↑ |

and also in concordance with the paracellular permeation of the macromolecular probes OGD10 and TRD78.

Especially LY and FM 1–43 are sensitive polar – and membrane markers, respectively, for the constitutive endocytosis taking place at the enterocyte brush border in the control situation. Although FM 4–64 inserted equally well as FM 1–43 into the epithelial membrane, its relatively slow endocytic uptake made it somewhat less useful as a predictor of PE action affecting this important cellular function. Maybe intuitively unlikely for a compound with a known transcellular mode of PE action, SDS effectively blocked endocytosis of all three probes. Epithelial transcytosis, i.e. apical endocytosis followed by basolateral exocytosis, can thus be ruled out as a possible mechanism of PE action of SDS. Studying other surfactant type of PEs using the mucosal explant system, we have previously observed a similar inhibitory effect on apical endocytosis.<sup>33–35</sup> From this, we conclude that although the mechanism of action of different types of membrane-interacting compounds may vary, they possess a similar functionality as PEs. Their common endocytosis-inhibiting effect is intriguing, and at present we are not certain of its cause. Perhaps it simply results from energy depletion by leakage of ATP or other small essential molecules/ions, but induced local changes in membrane lipid organization (for instance the balance between areas of high fluidity and lipid raft domains) might also be sufficient to interfere with endocytosis. The ultrastructural membrane changes seen with SDS (microvillus

microvesiculation and vesiculation along the lateral cell membranes) was also observed with other surfactant PEs and is suggestive of a functionally impaired membrane structure.

Contrary to SDS, EDTA had no observed inhibitory effect on apical endocytosis with any of the probes used. This seems remarkable, given the extreme disruption of the enterocyte apex caused by contraction of the actinomyosin ring, and the disorganized localization of the TWEEs in the bulging terminal web region is probably the result of the perturbed subapical actomyosin cytoskeleton.

As a surfactant SDS has the ability to insert into – and extract lipid molecules from the cell membrane, an action which may render the membrane leaky and allow diffusion of probes into the cell. This resulted in a diffuse staining of cytosol, easily distinguishable from the punctate apical endocytic uptake. However, only the probes of relatively low molecular weight, LY, and TRD3, entered the enterocytes by this route, suggesting that the pores generated in the lipid bilayer were too small to allow permeation of macromolecules.

Like SDS, EDTA action caused accumulation of low molecular weight probes (also including the lipophilic FM 1–43 and FM 4–64) in the enterocyte cytosol, a finding that may seem surprising for a PE lacking surfactant properties. Compared with SDS, which seemed to affect adjacent cells in a uniform manner, the effect of EDTA was patchy along the enterocytes of the epithelial surface. We speculate that the extreme bulging of the brush border region seen in some but not all enterocytes may be

responsible for this observation. Nevertheless, we must conclude that the ability to generate membrane leaks detectable by fluorescent probes is not a reliable criterion for distinguishing between PEs with paracellular -or transcellular modes of action.

In conclusion, this study was undertaken to assess the applicability of a mucosal explant system for studying transcellular – and paracellular actions of PEs. The actions of two selected PEs with well-known modes of action, transcellular-acting SDS and paracellular-acting EDTA, were distinct and clearly distinguishable in their labeling patterns obtained with the selection of polar – and lipophilic probes used. In future studies, we therefore recommend the mucosal explant system to be used as a simple experimental setup for screening new prospective agents for their mode of PE action.

## Acknowledgments

Karina Rasmussen is thanked for excellent technical assistance.

## Disclosure of potential conflicts of interest

No potential conflicts of interest to disclose.

## Funding

The study was supported by a grant from Læge Sofus Carl Emil Friis og hustru Olga Doris Friis legat.

## References

1. Maher S, Brayden DJ, Casattari L, Illum L. Application of permeation enhancers in oral delivery of macromolecules: an update. *Pharmaceutics*. 2019;11. doi:10.3390/pharmaceutics11020083.
2. Aungst BJ. Absorption enhancers: applications and advances. *AAPS J*. 2012;14:10–18. doi:10.1208/s12248-011-9307-4.
3. Fasinu P, Pillay V, Ndesendo VM, du Toit LC, Choonara YE. Diverse approaches for the enhancement of oral drug bioavailability. *Biopharm Drug Dispos*. 2011;32:185–209. doi:10.1002/bdd.750.
4. König J, Wells J, Cani PD, Garcia-Rodenas CL, MacDonald T, Mercenier A, Whyte J, Troost F, Brummer RJ. Human intestinal barrier function in health and disease. *Clin Transl Gastroenterol*. 2016;7:e196. doi:10.1038/ctg.2016.54.
5. France MM, Turner JR. The mucosal barrier at a glance. *J Cell Sci*. 2017;130:307–314. doi:10.1242/jcs.193482.
6. Maher S, Mrsny RJ, Brayden DJ. Intestinal permeation enhancers for oral peptide delivery. *Adv Drug Deliv Rev*. 2016;106:277–319. doi:10.1016/j.addr.2016.06.005.
7. Lichtenberg D, Robson RJ, Dennis EA. Solubilization of phospholipids by detergents. Structural and kinetic aspects. *Biochim Biophys Acta*. 1983;737:285–304.
8. Jones MN. Surfactants in membrane solubilisation. *Int J Pharma*. 1999;177:137–159.
9. Rodewald R, Kraehenbuhl JP. Receptor-mediated transport of IgG. *J Cell Biol*. 1984;99:159s–164s.
10. te Welscher YM, Chinnapen DJ, Kaoutzani L, Mrsny RJ, Lencer WI. Unsaturated glycosphingolipids as molecular carriers for mucosal drug delivery of GLP-1. *J Control Release*. 2014;175:72–78. doi:10.1016/j.jconrel.2013.12.013.
11. Garcia-Castillo MD, Chinnapen DJ, Lencer WI. Membrane transport across polarized epithelia. *Cold Spring Harb Perspect Biol*. 2017;9. doi:10.1101/cshperspect.a027912.
12. Citi S. Protein kinase inhibitors prevent junction dissociation induced by low extracellular calcium in MDCK epithelial cells. *J Cell Biol*. 1992;117:169–178.
13. Tomita M, Hayashi M, Awazu S. Comparison of absorption-enhancing effect between sodium caprate and disodium ethylenediaminetetraacetate in Caco-2 cells. *Biol Pharm Bull*. 1994;17:753–755.
14. Turner JR. Molecular basis of epithelial barrier regulation: from basic mechanisms to clinical application. *Am J Pathol*. 2006;169:1901–1909. doi:10.2353/ajpath.2006.060681.
15. Anderson JM, Van Itallie CM. Physiology and function of the tight junction. *Cold Spring Harb Perspect Biol*. 2009;1:a002584. doi:10.1101/cshperspect.a002584.
16. Turner JR, Angle JM, Black ED, Joyal JL, Sacks DB, Madara JL. PKC-dependent regulation of transepithelial resistance: roles of MLC and MLC kinase. *Am J Physiol*. 1999;277:C554–C562. doi:10.1152/ajpcell.1999.277.3.C554.
17. Madara JL, Marcial MA. Structural correlates of intestinal tight-junction permeability. *Kroc Found Ser*. 1984;17:77–100.
18. Turner JR. ‘Putting the squeeze’ on the tight junction: understanding cytoskeletal regulation. *Semin Cell Dev Biol*. 2000;11:301–308. doi:10.1006/scdb.2000.0180.
19. Lorenzen US, Hansen GH, Danielsen EM. Organ culture as a model system for studies on enterotoxin interactions with the intestinal epithelium. *Methods Mol Biol*. 2016;1396:159–166. doi:10.1007/978-1-4939-3344-0\_14.
20. Artursson P, Palm K, Luthman K. Caco-2 monolayers in experimental and theoretical predictions of drug transport. *Adv Drug Deliv Rev*. 2001;46:27–43.
21. Hansen GH, Sjöström H, Noren O, Dabelsteen E. Immunomicroscopic localization of aminopeptidase N in the pig enterocyte. Implications for the route of intracellular transport. *Eur J Cell Biol*. 1987;43:253–259.

22. Sjoström H, Noren O, Christiansen L, Wacker H, Semenza G. A fully active, two-active-site, single-chain sucrose-isomaltase from pig small intestine. Implications for the biosynthesis of a mammalian integral stalked membrane protein. *J Biol Chem.* **1980**;255:11332–11338.
23. Danielsen EM, Sjoström H, Noren O, Bro B, Dabelsteen E. Biosynthesis of intestinal microvillar proteins. Characterization of intestinal explants in organ culture and evidence for the existence of pro-forms of the microvillar enzymes. *Biochem J.* **1982**;202:647–654.
24. Booth AG, Kenny AJ. A rapid method for the preparation of microvilli from rabbit kidney. *Biochem J.* **1974**;142:575–581.
25. Laemmli UK. Cleavage of structural proteins during the assembly of the head of bacteriophage T4. *Nature.* **1970**;227:680–685.
26. Moore R, Carlson S, Madara JL. Rapid barrier restitution in an in vitro model of intestinal epithelial injury. *Lab Invest.* **1989**;60:237–244.
27. McCartney F, Gleeson JP, Brayden DJ. Safety concerns over the use of intestinal permeation enhancers: A mini-review. *Tissue Barriers.* **2016**;4:e1176822. doi:10.1080/21688370.2016.1176822.
28. Blikslager AT, Moeser AJ, Gookin JL, Jones SL, Odle J. Restoration of barrier function in injured intestinal mucosa. *Physiol Rev.* **2007**;87:545–564. doi:10.1152/physrev.00012.2006.
29. Louvard D, Kedinger M, Hauri HP. The differentiating intestinal epithelial cell: establishment and maintenance of functions through interactions between cellular structures. *Annu Rev Cell Biol.* **1992**;8:157–195. doi:10.1146/annurev.cb.08.110192.001105.
30. Cao X, Surma MA, Simons K. Polarized sorting and trafficking in epithelial cells. *Cell Res.* **2012**;22:793–805. doi:10.1038/cr.2012.64.
31. Hanani M. Lucifer yellow - an angel rather than the devil. *J Cell Mol Med.* **2012**;16:22–31. doi:10.1111/j.1582-4934.2011.01378.x.
32. Gopalakrishnan S, Pandey N, Tamiz AP, Vere J, Carrasco R, Somerville R, Tripathi A, Ginski M, Paterson BM, Alkan SS. Mechanism of action of ZOT-derived peptide AT-1002, a tight junction regulator and absorption enhancer. *Int J Pharma.* **2009**;365:121–130. doi:10.1016/j.ijpharm.2008.08.047.
33. Danielsen EM, Hansen GH. Intestinal surfactant permeation enhancers and their interaction with enterocyte cell membranes in a mucosal explant system. *Tissue Barriers.* **2017**;5:e1361900. doi:10.1080/21688370.2017.1361900.
34. Danielsen EM, Hansen GH. Impact of cell-penetrating peptides (CPPs) melittin and HIV-1 Tat on the enterocyte brush border using a mucosal explant system. *Biochim Biophys Acta.* **2018**;1860:1589–1599. doi:10.1016/j.bbame.2018.05.015.
35. Danielsen EM, Hansen GH. Probing the action of permeation enhancers sodium cholate and N-dodecyl-beta-D-maltoside in a porcine jejunal mucosal explant system. *Pharmaceutics.* **2018**;10. doi:10.3390/pharmaceutics10040172.
36. Hansen GH, Rasmussen K, Niels-Christiansen LL, Danielsen EM. Endocytic trafficking from the small intestinal brush border probed with FM dye. *Am J Physiol Gastrointest Liver Physiol.* **2009**;297:G708–G715. doi:10.1152/ajpgi.00192.2009.
37. Danielsen EM, Hansen GH. Generation of stable lipid raft microdomains in the enterocyte brush border by selective endocytic removal of non-raft membrane. *PLoS One.* **2013**;8:e76661. doi:10.1371/journal.pone.0076661.
38. Bolte S, Talbot C, Boutte Y, Catrice O, Read ND, Satiat-Jeunemaitre B. FM-dyes as experimental probes for dissecting vesicle trafficking in living plant cells. *J Microsc.* **2004**;214:159–173. doi:10.1111/j.0022-2720.2004.01348.x.
39. Danielsen EM. Probing endocytosis from the enterocyte brush border using fluorescent lipophilic dyes: lipid sorting at the apical cell surface. *Histochem Cell Biol.* **2015**;143:545–556. doi:10.1007/s00418-014-1302-2.